

Conjugated Polymer Network Films from Precursor Polymers: Electrocopolymerization of a Binary Electroactive Monomer Composition

Prasad Taranekar, Akira Baba, Timothy M. Fulghum, and Rigoberto Advincula*

Department of Chemistry, University of Houston, Houston, Texas 77204-5003

Received January 1, 2005; Revised Manuscript Received February 28, 2005

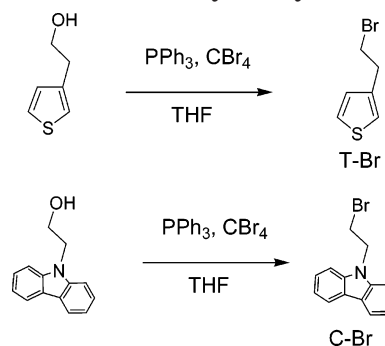
ABSTRACT: We report the synthesis and electropolymerization of a precursor polymer with a binary molecular composition of thiophene and carbazole electroactive groups to form ultrathin films of conjugated polymer networks (CPN) on flat indium tin oxide (ITO) substrates. In the past we have demonstrated the precursor polymer approach based on a single pendant electroactive group. In this work, we describe the interesting electrocopolymerization mechanism and properties of precursor polymers prepared with two different types of pendant electroactive groups (statistical copolymer) and compared behavior to their respective homopolymers. The presence of a smaller amount of carbazole induces the electropolymerization of the higher oxidation potential thiophene units via the reaction of a radical cation and a neutral molecule pathway. These electrochemically generated thin films gave unique optical, electrochemical, and morphological properties as a function of composition. The film properties were investigated by cyclic voltammetry (CV), spectroelectrochemistry, EQCM, atomic force microscopy (AFM), and X-ray photoelectron spectroscopy (XPS).

Introduction

Conjugated polymers are widely studied polymer systems. These materials have received much attention due to their potential applications in light-emitting devices, field effect transistors, charge storage devices, photodiodes, sensors, resist materials, etc.¹ Substituted polythiophenes and poly(*N*-alkyl-3,6-carbazoles) are materials of great interest as they can act as hole transport materials when utilized in organic light-emitting diode (OLED) applications.² They can be synthesized both chemically and electrochemically.³ A number of groups have in fact reported the copolymerization of carbazole and thiophenes and their application as OLED materials.^{3,16,22} Their application to electrografting methods have been reported but with ill-defined electrochemical mechanisms.^{3,27} It is well-known that introducing substituents to an electropolymerizable monomer increases the overall oxidation potential such that it can become difficult to electrochemically deposit without decomposing the polymer at the same time. In the past this problem was overcome by extending the conjugation length of the monomer to a dimer, trimer, etc., resulting in a significant reduction of the overall oxidation potential.⁴ In the present work, the presence of a very small amount of carbazole triggers the electropolymerization of the higher oxidation potential thiophene units and thus opening an alternative pathway to polymerize higher oxidation potential electroactive monomers without having to do extensive synthesis of dimers, trimers, etc.

In our previous work, we have demonstrated the viability of the “precursor polymer” approach based on single pendant electroactive monomer group using various polymer backbones.⁵ This involved the tethering of electroactive monomers to a polymer backbone which results in the formation of electrooptically active conjugated polymer network (CPN) or cross-linked films after electropolymerization.^{1d,5} These materials have been reported to be useful for device applications.⁶ While a number of homopolymers and copolymers have been reported which contain one type of tethered monomer,

Scheme 1. Synthetic Scheme for the Monomers Used in Precursor Polymer Synthesis

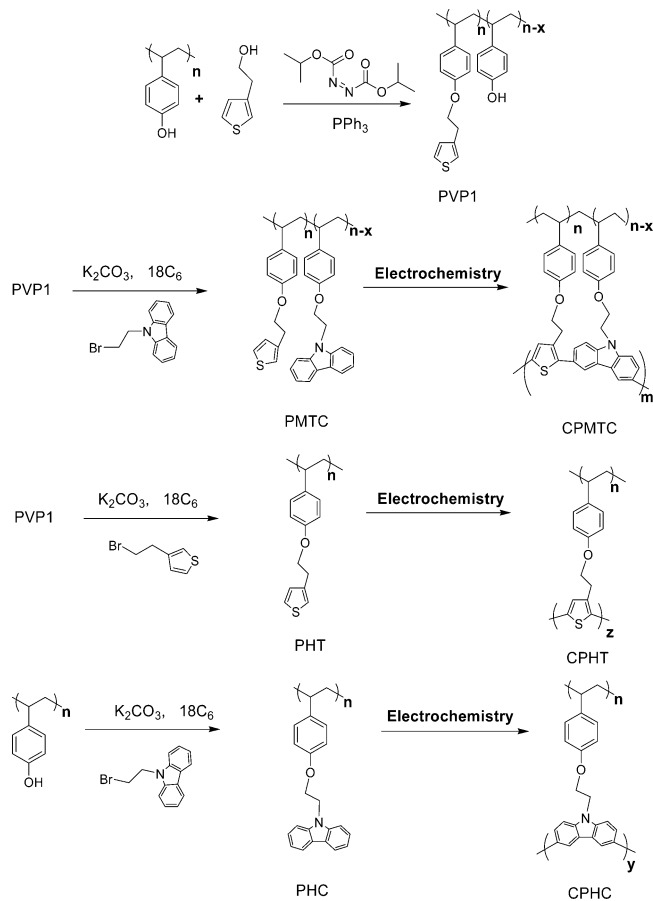


none has been reported for binary tethered monomer compositions pendant on a polymer backbone.

Here we report the formation of ultrathin films of a CPN based on a precursor polymer with thiophene and carbazole electroactive monomers grafted onto a poly(4-vinylphenol) backbone (Scheme 2). The poly(4-vinylphenol) backbone was chosen because of its relatively high glass transition temperature, chemical inertness, and optical transparency. Changes in the optical properties of conjugated polymers can be driven by a delicate balance between repulsive steric interactions and attractive interchain and (or, interchain, due to chain folding) interactions with its alkyl substituent (or non-conjugated component).⁷ In addition, poly(*N*-vinylcarbazole) and other *N*-substituted carbazole with PVP-like backbones such as poly(9-(4-ethynylphenyl)carbazole) and poly(*N*-(*p*-ethynylbenzoyl)carbazole) polymers are materials of interest in terms of their redox activity, porosity, and doping–dedoping reversibility.⁸ We have used this doping–dedoping reversibility to tune the work function of a cross-linked poly(vinylcarbazole) (PVK) film on ITO in a multilayer OLED device in order to improve hole-injection/transport properties.^{6b}

It is interesting to study both thiophene and carbazole monomers because they can form unique copolymer compositions, polymerization mechanisms, and electro-

Scheme 2. Synthetic Scheme for the Cross-Linked Homopolymers and Copolymer from Their Respective Precursors



optical applications.^{3,16,22,27} The copolymer bearing a statistical binary electroactive monomer composition will have properties in between that of polythiophenes and polycarbazoles. The ability of one monomer to polymerize in the presence of another monomer has also been reported in the past.⁹ Both *N*-ethylcarbazole and *N*-phenylcarbazole produce noncoherent electropolymerized films,¹⁰ which can be overcome by the introduction of thiophene into the copolymer structure, resulting in stable, optically clear, and coherent conducting polymer films.

In this work, we investigated the precursor polymer route for these two monomers by depositing films using anodic electropolymerization methods. We describe the synthesis, film preparation, and characterization in terms of in-situ mass change, electrooptical properties during and after electropolymerization, and surface morphological behavior for the copolymers. An interesting electrocopolymerization mechanism was observed along with tunable electrooptical properties for these monomers. The electrochemical copolymerization behavior was compared to their individual homopolymer analogues. Studies were also made involving their mixtures and comonomer deposition (monomer directly introduced in solution). The possibilities of intramolecular "template" electropolymerization vs intermolecular cross-linking reactions were discussed.

Experimental Section

Instrumentation. NMR was done on a General Electric QE 300 spectrometer (¹H 300 MHz). UV-vis was recorded using Agilent 8453 spectrometer. The SEC analysis was

performed using a Viscotek 270 quad detector equipped with VE3210 UV/vis detector and VE3580 RI detector. The columns used for finding size exclusion chromatography (SEC) number-average molecular weight ($M_{n,sec}$) type are G3000H_{HR} and GHM_{HR}-M viscogel. All FTIR measurements were done using a Digilab FTS 7000 step scan spectrometer. Cyclic voltammetry was performed on an Amel 2049 potentiostat and power lab/4SP system with a three-electrode cell. In all the measurements the counter electrode was platinum wire, and the indium tin oxide (ITO) was used as a working electrode and was pretreated with RCA recipe (H₂O/H₂O₂/NH₃::15.1 g/26.6 g/8.57 g).¹¹ The QCM apparatus, probe, and crystals are available from MAXTEK Inc. The diameter of the polished AT-cut QCM crystals (5 MHz) was 13 mm. The data acquisition was done using a RQCM (Research Quartz Crystal Microbalance, MAXTEK, Inc.) system equipped with an inbuilt phase lock oscillator and the RQCM Data-Log Software. The gold electrodes were cleaned with a plasma etcher (Plasmod, March). To measure the polymer adsorption, the inert probe was first immersed in methylene chloride until a stable frequency was obtained. Atomic force microscopy (AFM) imaging was examined in ambient conditions with a PicoSPM II (PicoPlus, Molecular Imaging) in the Magnetic AC mode (MAC mode). MAC mode uses a magnetic field to drive a magnetically coated cantilever in the top-down configuration. Type II MAC levers with a spring constant of 2.8 nN/m with about 10 nm tip radius were used for all scans. A contact mode was used for surface profilometry measurements using a cantilever (Nanosensor) of spring constant 0.07–0.4 nN/m and resonance frequency of 10–17 kHz. X-ray photoelectron spectroscopy (XPS) was carried out on a Physical Electronics 5700 instrument with photoelectrons generated by the nonmonochromatic Al K α irradiation (1486.6 eV). Photoelectrons were collected at a takeoff angle of 45° using a hemispherical analyzer operated in the fixed retard ratio mode with an energy resolution setting of 11.75 eV. The binding energy scale was calibrated prior to analysis using the Cu 2p_{3/2} and Ag 3d_{5/2} lines. Charge neutralization was ensured through cobombardment of the irradiated area with an electron beam and the use of the nonmonochromated Al K α source. This placed the adventitious C 1s peak at a binding energy of 284.6 ± 0.2 eV.

Reagents. Poly(4-vinylphenol) (M_w = 11 430) was purchased from Aldrich, and all other chemicals used were from Fischer Chemical Co. The ITO was used as a working electrode and was pretreated with RCA recipe (H₂O/H₂O₂/NH₃::15.1 g/26.6 g/8.57 g). All solvents were distilled and dried properly before use.

Synthesis of 3-(2-Bromoethyl)thiophene (T-Br) (Scheme 1). A solution of 4.15 g (12.5 mmol) of CBr₄ in 15 mL THF was added dropwise to an ice cold magnetically stirred solution containing 1.28 g (10.0 mmol) 2-thiophen-3-ylethanol and 3.92 g (15.0 mmol) of PPh₃ dissolved in 10 mL THF. After addition was complete, the mixture was stirred for an additional 6 h, whereupon the solvent was removed under vacuum. The concentrate was then dissolved in methylene chloride and washed with aqueous NaOH solution. The organic layer was then extracted again thoroughly washed with water and was dried over Na₂SO₄. The residue was purified by flash column chromatography with hexane as an eluent to give 1.6 g (83.7%) of the bromide as a colorless oil. ¹H NMR (δ ppm in CDCl₃): 7.16 (q, 1H), 7.084–6.99 (m, 2H), 3.58 (t, 2H), 3.21 (t, 2H).

Synthesis of 9-(2-Bromoethyl)-9H-carbazole (C-Br) (Scheme 1). A solution of 4.15 g (12.5 mmol) of CBr₄ in 15 mL THF was added dropwise to an ice cold magnetically stirred solution containing 2.11 g (10.0 mmol) 2-carbazol-9-ylethanol and 3.92 g (15.0 mmol) of PPh₃ dissolved in 10 mL THF. After addition was complete, the mixture was stirred for an additional 10 h, whereupon the solvent was removed under vacuum. The concentrate was then dissolved in methylene chloride and washed with aqueous NaOH solution. The organic layer was then extracted again thoroughly washed with water and was dried over Na₂SO₄. The residue was purified by flash column chromatography with hexane as an eluent to give 2.1 g (76.6%) of the bromide as white crystals. ¹H NMR (δ ppm in

CDCl₃): 8.20 (d, 2H), 7.62–7.52 (m, 4H), 7.39 (m, 2H), 4.81 (t, 2H), 3.78 (t, 2H).

Synthesis of Poly([3-(2-(4-vinylphenoxy)ethyl)thiophene]-co-4-vinylphenol) (PVP1) (Scheme 2). A 250 mL round-bottom flask was charged with poly(4-vinylphenol) (0.75 g), 2-thiophen-3-ylethanol (0.66 g), and triphenylphosphine (2.09 g) in 20 mL of distilled THF under nitrogen. At 0 °C a 5 mL THF solution of diisopropylazodicarboxylate (DIAD, 1.21 g) was poured in the reaction mixture. After 24 h water was added to quench the reaction, and then solvent was subjected to vacuum. The reaction mixture was redissolved in methylene chloride and extracted from water. The solvent was then removed under vacuum, and the resulting reaction mixture was dropwise added to cold diethyl ether under vigorous stirring. The polymer was obtained as a white precipitate. The obtained polymer was redissolved in methylene chloride and was reprecipitated in cold methanol. This process was repeated several times until no other impurities were observed. Proton NMR was done on the vacuum-dried product, and in 5% confidence limit based on the integration we propose 68% grafting of thiophene units. ¹H NMR (δ ppm in CDCl₃): 7.20–7.00 (b, 1.99H), 6.54 (b, 4H), 5.33 (b, 0.6H), 4.04 (b, 1.33H), 3.029 (b, 1.30H), 1.98–0.63 (b, 6H).

Synthesis of Poly([3-(2-(4-vinylphenoxy)ethyl)thiophene]-co-9-[2-(4-vinylphenoxy)ethyl]-9H-carbazole) (PMTC) (Scheme 2). In a solution of 15 mL of distilled acetone, 0.255 g (1.70 mmol) of PVP1, 1.38 g (10 mmol) of K₂CO₃, 0.066 g (0.25 mmol) of 18C₆, and 0.246 g (0.9 mmol) of C-Br (9-(2-bromoethyl)-9H-carbazole) were all mixed at once and refluxed under nitrogen for 48 h. The solvent was removed under vacuum, and the reaction mixture was then poured in water and extracted with methylene chloride. The solvent was removed under vacuum, and the resulting reaction mixture was dropwise added to cold solution of hexane under vigorous stirring. A white precipitate was recovered dried under vacuum and was confirmed by NMR. The SEC analysis showed $M_n = 34\,742$ Da as the number-average molecular weight. The NMR showed more than 95% of overall grafting. ¹H NMR (δ ppm in CDCl₃): 8.135–7.00 (b, 5.5H), 6.54 (b, 4H), 4.51–4.04 (b, 3H), 3.029 (b, 1.3H), 1.98–0.63 (b, 6H). The FTIR (KBr) in wavenumber (cm⁻¹) shows¹² (Ph–O–C) 810–850, (C–S)_{ring} 950, (Ph–O–C) 1210 (br, s), aromatic (C–H) 1250–1270 (s), (C–N)_{ring} 1250–1380, aromatic (C–H) 1470–1525 (s), thiophene (C–C)_{ring} 1580 (s), aromatic (C–H) 1590–1625, carbazole (C=C)_{ring} 1650 (s), thiophene (C=C)_{ring} 1746 (s), ν_s (CH₂) 2860 (br), ν (CH) 2910 (br), ν_{as} (CH₂) 2932 (br), carbazole (C–N)_{ring} 3000 (br, s), thiophene (C–C)_{ring} 3310 (w), (Ph–O–H) 3400 (br, w).

Synthesis of Poly([3-(2-(4-vinylphenoxy)ethyl)thiophene] (PHT) (Scheme 2). In a solution of 20 mL of distilled acetone, 0.255 g (1.70 mmol) of PVP1, 1.38 g (10 mmol) of K₂CO₃, 0.066 g (0.25 mmol) of 18C₆, and 0.4 g (2.55 mmol) of T-Br (3-(2-bromoethyl)thiophene) were all mixed at once and refluxed under nitrogen for 48 h. The solvent was removed under vacuum, and the reaction mixture was then poured in water and extracted with ethyl acetate. The organic extract was dried over Na₂SO₄. After filtration the organic extract was concentrated. The concentrate was then added dropwise in hexane to give a white precipitate, which was then filtered and washed thoroughly again with diethyl ether. The precipitate was dried under vacuum, and the product was confirmed by NMR. The NMR showed more than 80% grafting. The SEC analysis showed $M_n = 16\,257$ Da as the number-average molecular weight. ¹H NMR (δ ppm in CDCl₃): 7.20–7.00 (b, 2.6H), 6.54 (b, 4H), 5.33 (b, 0.2H), 4.04 (b, 1.60H), 3.029 (b, 1.60H), 1.98–0.63 (b, 6H). The FTIR (KBr) in wavenumber (cm⁻¹) shows¹² (Ph–O–C) 810–850, (C–S)_{ring} 950, (Ph–O–C) 1210 (br, s), aromatic (C–H) 1250–1270 (s), aromatic (C–H) 1470–1525 (s), thiophene(C–C)_{ring} 1580 (s), aromatic (C–H) 1590–1625, thiophene (C=C)_{ring} 1746 (s), ν_s (CH₂) 2860 (br), ν (CH) 2910 (br), ν_{as} (CH₂) 2932 (br), thiophene (C–C)_{ring} 3310 (w), (Ph–O–H) 3400 (br, w).

Synthesis of Poly[9-[2-(4-vinylphenoxy)ethyl]-9H-carbazole] (PHC) (Scheme 2). In a solution of 20 mL of distilled acetone, 0.255 g (1.70 mmol) of PVP1, 1.38 g (10 mmol) of K₂CO₃, 0.066

g (0.25 mmol) of 18C₆, and 0.7 g (2.55 mmol) of C-Br (9-(2-bromoethyl)-9H-carbazole) were all mixed at once and refluxed under nitrogen for 72 h. The solvent was removed under vacuum, and the reaction mixture was then poured in water and extracted with ethyl acetate. The organic extract was dried over Na₂SO₄. After filtration the organic extract was concentrated. The concentrate was then added dropwise in hexane to give a white precipitate, which was then filtered and washed thoroughly again with diethyl ether. The precipitate was dried under vacuum and the product was confirmed by NMR. The NMR showed more than 95% of grafting. SEC analysis failed on this polymer even after repeated trials. ¹H NMR (δ ppm in CDCl₃): 8.14 (b, 2H), 7.33 (b, 6H), 6.54 (b, 4H), 4.51–4.04 (b, 4H), 1.98–0.63 (b, 6H). The FTIR (KBr) in wavenumber (cm⁻¹) shows¹² (Ph–O–C) 810–850, (Ph–O–C) 1210 (br, s), aromatic (C–H) 1250–1270 (s), (C–N)_{ring} 1250–1380, aromatic (C–H) 1470–1525 (s), aromatic (C–H) 1590–1625, carbazole (C=C)_{ring} 1650 (s), ν_s (CH₂) 2860 (br), ν (CH) 2910 (br), ν_{as} (CH₂) 2932 (br), carbazole (C–N)_{ring} 3000 (br, s), (Ph–O–H) 3400 (br, w).

Electrochemical Synthesis of Cross-Linked Polymers (CPHC/CPHT/CPMTC). The precursor polymers were electropolymerized using cyclic voltammetry techniques. In a three-electrode cell 0.1 M tetrabutylammonium hexafluorophosphate (TBAP) as supporting electrolyte and 10 mM of each polymer were dissolved in 5 mL of methylene chloride separately. The electropolymerization of the each precursor polymer was performed by sweeping the voltage at a scan rate of 20 mV/s from 0 to 1.1 V in the case of CPHC, 1.5 V for CPMTC, and up to 1.6 V was used for CPHT against Ag/AgCl as a reference electrode and platinum as a counter electrode. The ITO was used as a working electrode and also as a substrate.

Results and Discussion

Electropolymerization. To first test their ability to form thin films, the precursor polymers (homopolymer and copolymer) were electropolymerized and deposited on the ITO substrate. Their chemical structures are outlined in Scheme 2. Before investigating the electrochemical behavior of the cross-linked copolymer CPMTC, we first synthesized and studied the cross-linked CPHT and CPHC homopolymers. The CPHT homopolymer is poorly electropolymerized despite several trials attempted within a range of applied potentials. Under visual observation, it started to form a thick white layer from the first cycle, and if the potential is exceeded beyond 1.6 V, the film started to degrade as seen from the appearance of the film turning brown in color. We believe this happens mainly because of two reasons: (1) The first is the low grafting density (~80%) of thiophene and the remaining phenolic groups, which rapidly physisorbs and pacifies the ITO surface. (2) Another reason is that the thiophene monomer oxidation is very high compared to its polymer. In this case, the introduction of the nonconducting polymer backbone further increases the oxidation potential; therefore, high applied potentials causes degradation of the polymer.¹³ This is in contrast to the CPHC homopolymer, which electropolymerized readily at a lower onset of oxidation potential of 0.7 V (Figure 1a).^{6b} This should occur primarily at the carbazole 3,6-position vs the lower electron density 2,7-position which is accessible only via metal-mediated coupling reactions.^{3,8}

Thus, for the CPHT precursor polymer, it is of high interest to determine electropolymerizability when another monomer, carbazole, is present in the same polymer backbone.^{3,9,16} By introducing the carbazole monomer with a lower oxidation potential and ensuring high grafting density close to 100%, copolymerization can potentially extend the conjugation of the thiophene

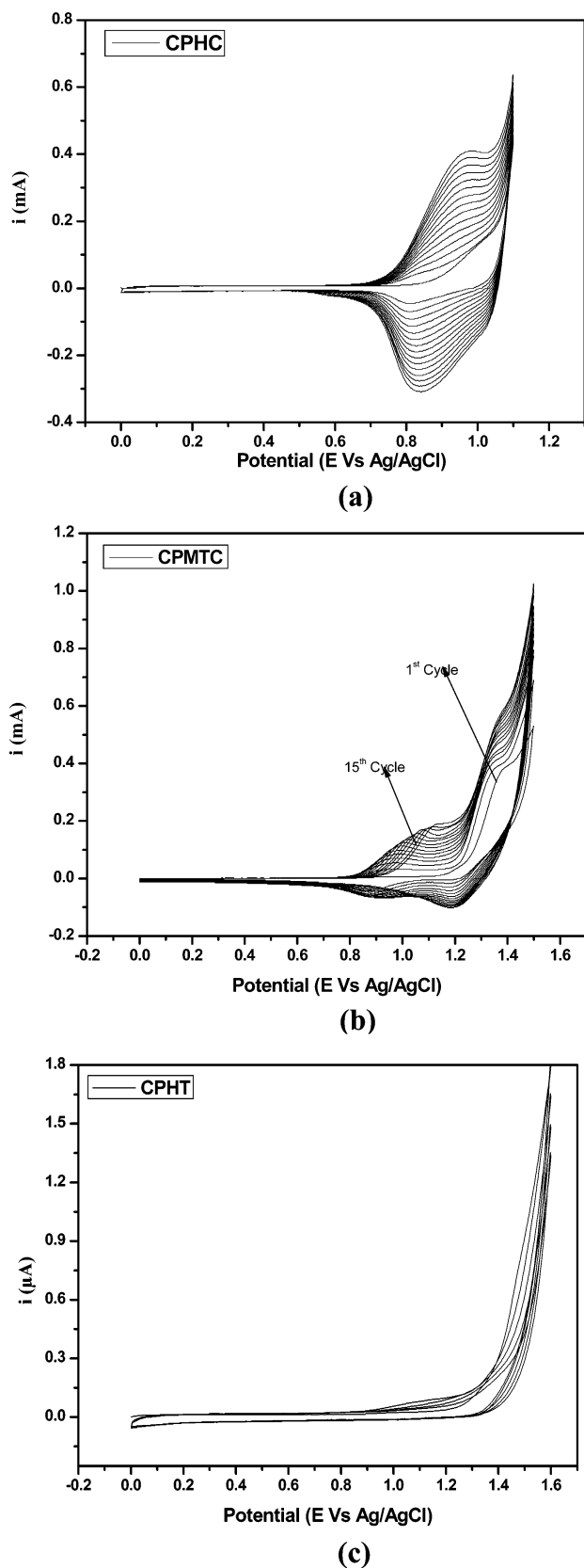


Figure 1. Cyclic voltammetry on ITO for precursor polymers: (a) CPHC, (b) CPMTc, and (c) CPHT.

monomer, resulting in a significant reduction in the overall oxidation potential of the precursor polymer. Increased planarity along the polymer chain caused by the coupling of thiophene and carbazole units can also lower the oxidation potential.¹⁴

In the past Sarac et al.¹⁶ have demonstrated that a high feed ratio of thiophene to carbazole is required to enhance effective copolymerization. Therefore, we incorporated more thiophene units than the carbazole in the precursor copolymer to facilitate electrocopolymerization. The CV curves are shown in Figure 1. In CPMTc (Figure 1b) after 15 cycles we observed two anodic oxidation peaks E_{pa1} and E_{pa2} at 1.14 and 1.37 V, respectively, with their corresponding reduction peak potentials E_{pc1} and E_{pc2} occurring at 0.89 and 1.19 V. It is interesting to observe that after five cycles the E_{pc1} value does not increase; instead, we see a constant growth in E_{pc2} values only, suggesting the formation of polythiophene.¹⁶ Thus, on an electrode surface, although the percentage of incorporated carbazole was low, the polymerization of thiophene only becomes facile due to the presence of carbazole. The fact that we observe a broad oxidation peak in the range of the oxidation potentials of the two monomers suggests that the electrocopolymerization process has taken place. A smaller amount of the carbazole triggers the electropolymerization of the thiophene units. This fact is highlighted since the statistical ratio of thiophene to carbazole in the precursor polymer is almost 2:1. Note that the possibility of α - α , α - β , and β - β reaction on the thiophene units cannot be easily distinguished by CV methods alone, although on the basis of electron density of the C centers, the α - α coupling is expected to predominate.³ Similarly, the 3,6-position coupling is expected to predominate vs the 2,7-positions of the carbazole.⁸

To further understand the CPMTc polymer behavior, we studied the copolymerization of blends formed by mixing two homopolymers with different feed ratios, as seen in Figure 2. The cross-linked copolymer 27-(cbz-co-th) comprised a mixing feed ratio of 25:75 PHC:PHT. As shown in Figure 2a, two cathodic peaks E_{pc1} and E_{pc2} at 0.73 and 1.1 V, respectively, were observed. The absence of the 1.1 V in the case of CPHC-1.6 polymer (Figure 2a) but present in the copolymer 27-(cbz-co-th) suggests that this peak is primarily due to polythiophene formation. This observation supports our argument of polythiophene formation as stated in the case of CPMTc. In the case of copolymer 72-(cbz-co-th) formed upon mixing the two homopolymers PHC:PHT in the ratio of 75:25 (Figure 2b), we observed similar cathodic and anodic peak potentials to that of copolymer 27-(cbz-co-th) but with different peak current ratios. The peak cathodic current I_{pc1} was found to be twice that of I_{pc2} in the case of copolymer 72-(cbz-co-th), but both of the I_{pc} values were found to be equal for that of copolymer 27-(cbz-co-th). Both these copolymers were found to be optically opaque as compared to the CPMTc copolymer, which was optically clear. This is perhaps due to the influence on film morphology with higher polymer backbone (polystyrene) content on the mixture. It should be noted that the copolymer formed from the mixture of the two individual homopolymers bear twice the molar content of the "nonconducting" PVP backbone as compared to that of CPMTc. It should be possible to distinguish synergistic, nonsynergistic, or additive electrochemical behavior by investigating more composition ratios.

Spectroelectrochemical Studies. Figure 3a shows the in-situ spectroelectrochemical studies of the CPHC homopolymer cross-linked film analyzed after stepwise

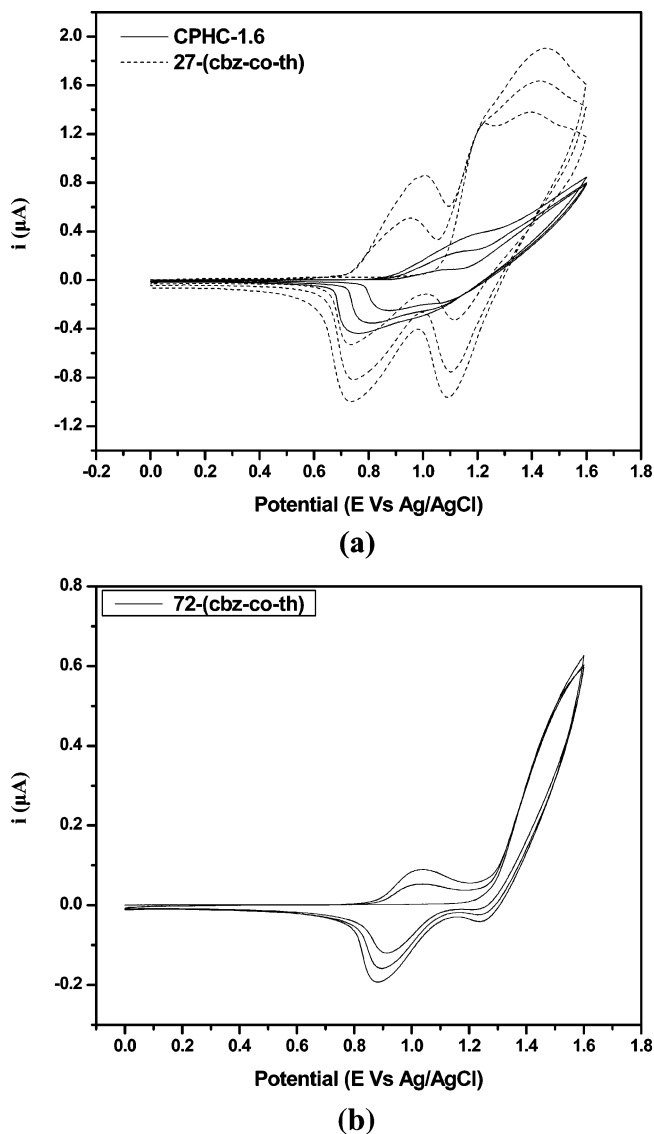


Figure 2. Cyclic voltammetry on ITO for copolymers formed upon mixing the two homopolymers up to three cycles: (a) copolymer 27-(cbz-co-th) and CPHC polymerized up to 1.6 V; (b) copolymer 72-(cbz-co-th).

oxidation up to 1.1 V and then brought to its neutral state at 0 V. As the applied potential is increased, the absorption in the visible due to the $\pi-\pi^*$ transition bleaches.¹⁷ In CPHC, which contains carbazole units, an absorption peak is visible at 310 nm and a shoulder at 335 nm is observed, which are typically due to the $\pi-\pi^*$ transition in polycarbazole.^{18,19} In the case of spectroelectrochemical observation done under monomer free conditions, we observed that with increasing voltage the peak at 310 nm bleaches and the film starts to turn green giving rise to two new peaks at 418 and 699 nm during the stepwise oxidation of the cross-linked polymer film. The peaks at 310, 418, and 699 nm have been understood to arise from the valence band to conduction band, polaron bonding level to π^* conduction band, and bonding level to antibonding state of polaron transitions, respectively.^{20,21}

In the case of cross-linked CPMTc the polymer peak due to the $\pi-\pi^*$ transition appears at 366 nm (Figure 3b). After stepwise variation in the potentials from 0–1.5 V and back to 0 V, we observe that the $\pi-\pi^*$ transition bleaches at 1.5 V and a new peak appears at

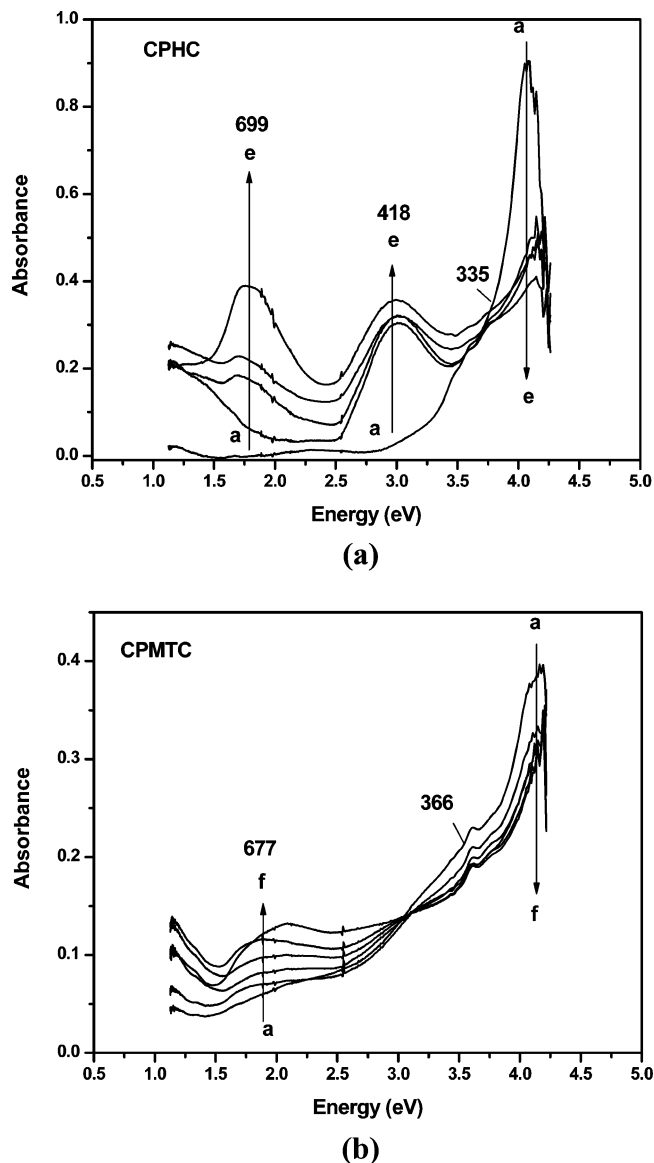
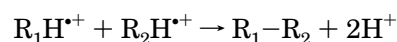


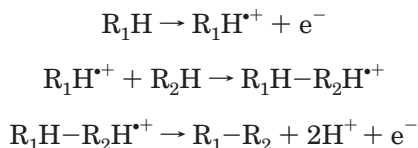
Figure 3. Spectroelectrochemical analysis performed in 0.1 M TBAP/ CH_2Cl_2 on (a) PHC polymer with (a) 0, (b) 0.8, (c) 0.9, (d) 1.0, and (e) 1.1 V vs Ag/AgCl and on (b) PMTC polymer with (a) 0, (b) 0.8, (c) 1.0, (d) 1.1, (e) 1.2, and (f) 1.4 V vs Ag/AgCl.

677 nm. This peak around 677 nm is attributed to the formation of a copolymer of thiophene and carbazole.²² The absence of the absorbance at 418 nm in the case of CPMTc compared to CPHC indicates that individual carbazole polaronic transitions are not occurring, and this optical behavior can therefore be attributed to the carbazole intervention in the thiophene to form a true copolymer. Nevertheless, the possibility of carbazole–carbazole oligomerization cannot be discounted.⁹ In general, with copolymerization, the reaction of two radical cation species results in dimer formation⁹



while the reaction of a radical cation with the neutral

comonomer results in copolymer formation:



In this case, this latter mechanism is predominant in the presence of the lower oxidation potential carbazole with thiophene. The neutral state (dedoped) of both cross-linked CPHC and CPMTTC polymers are colorless.

It should be noted that the combination of two monomers in the precursor copolymers or the blend of the homopolymers results in the statistical possibilities of thiophene–thiophene, carbazole–carbazole, and thiophene–carbazole electropolymerizations. The case can also be added for two other limiting cases: intramolecular reaction (with the same chain) which can lead to a ladder-type structure or intermolecular reactions (with another chain), which leads to a highly cross-linked or network architecture. The former gives way to a “templating” of the electropolymerization process where the monomers are already connected to the same polymer backbone. The latter results in network cross-linking of individual polymer chains through the pendant monomers. These possibilities are not easily distinguished in the current system although the higher probability of intermolecular cross-linking is more probable because of (a) an insoluble film is formed, (b) the appearance of electropolymerized CPHT species only in the presence of carbazole monomers, and (c) the blends of the homopolymers resulted in electropolymerization, which is not possible for the PHT alone. Future studies can be made using labeled monomers or even a pre-formed polymer backbone template that favor intrachain ladder-type reactions, e.g., stiff polymer chains.

EQCM. The mass deposition per cycle and ion transport properties were studied by electrochemical quartz crystal microbalance (EQCM) during the electrochemical polymerization. While it is true that viscoelastic effects do play a role in frequency changes when characterizing films by EQCM, it has been shown that EQCM is an effective tool for characterizing sufficiently thin films.²³ For thin films (where the film thickness is much less than the wavelength of the piezoelectrically launched shear waves) a simplified form of the mass–frequency relation can be used. From the well-known Sauerbrey equation, the frequency shift ΔF (Hz) is a function of several parameters in the QCM setup.²⁴

Upon application of potential (see Supporting Information Figure 1a,b), the deposited mass increases due to the oxidative CPHC or CPMTTC deposition, in addition to the mass associated with hexafluorophosphate counterions. After sweeping the potential back to 0 V, the polymer is reduced to the neutral form, and a loss of mass on the crystal occurs due to predominant transport of anions out of the polymer. It is interesting to note that the mass loss in the region corresponding to anion departure from the film upon reduction is identical for each scan in the case of CPMTTC as compared to CPHC polymer. Both films as seen from Figure 4a show almost uniform rate of growth with time as observed by the periodic changes in their frequency values. Figure 4b shows the change of mass per cycle. Since the applied potentials are different for each case, it is hard to make conclusions regarding any autoacceleration effects from

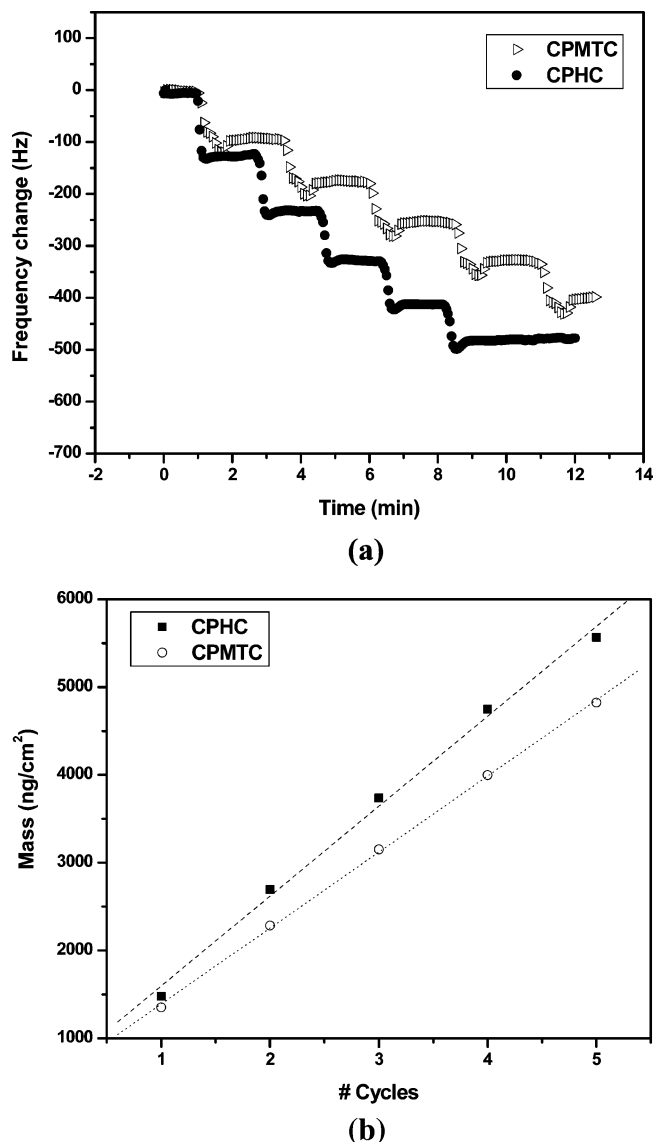


Figure 4. EQCM studies for the polymers PHC and PMTC during electropolymerization.

the carbazole during the electropolymerization. However, it should be noted that both CPMTTC and CPHC polymers behave ideally in terms of the mass deposition/cycle, giving a homogeneous film growth.

Band Gap/Scan Rate Studies. The redox behavior of the CPMTTC film was investigated by cyclic voltammetry with films prepared by electropolymerization up to five cycles. The polymer film showed a reversible p-doping and a pseudo-reversible n-doping. The anodically scanned cyclic voltammograms (see Supporting Information, Figure 2a) showed an oxidation onset of 0.65 V and gave a peak at 0.89 V and a corresponding reduction peak at 0.68 V. The cathodic wave during n-doping had an onset of -1.36 V and gave a peak at -2.22 V. The electrochemical energy gap, ΔE° ($\Delta E^\circ = \Delta E^\circ_{\text{ox}} - \Delta E^\circ_{\text{red}}$), was found to be 3.12 V, which is slightly lower than the optical energy band gap of 3.38 eV (366 nm).

At this point, it is interesting to investigate the kinetics of the redox reaction of the adsorbed layer, which was performed by varying the scan rate from 20 up to 100 mV/s (Supporting Information, Figure 2b). The electrochemical conditions were kept similar as described earlier for the band gap studies. An analysis of

the CV peak current as a function of scan rate in monomer-free solution shows a linear response to ion transport (inset, Figure 2b). This indicates a diffusion-controlled process for ion transport on the adhered polymer to the electrode surface. In this case, if the mass transfer is diffusion-limited, I_{pa} is proportional to the scan rate^{1/2}.

XPS Studies. Figure 5 shows the high-resolution XPS spectra CPHT, CPHC, and CPMTC cross-linked polymers on ITO. The absence of fluorine (F 1s) and phosphorus (P 2p) indicates that the films were completely reduced, and therefore no counterions were detected. The CPHT cross-linked polymer primarily physisorbs on the surface of ITO because of the phenolic group, and therefore we observed very poor sulfur intensity. Instead, we observed a broad band with a very high intensity of O 1s (Figure 5d). The CPHC and CPMTC cross-linked polymers gave a single peak around 532.8 eV, which can be attributed to C–O–C bonds. The observation of only nitrogen peak in the case of CPHC and both nitrogen and sulfur peaks in CPMTC confirms the presence of the cross-linked films on the electrode. Table 1 summarizes the presence of carbon, nitrogen, and sulfur elements, their binding energies (BE), and their relative atomic concentrations (AC) present in the films. In all the quantitative analysis the theoretical value is assumed on the basis of 100% grafting and then compared to the experimental value. As an example for CPHC, the theoretical values are O/N = 1.14 and C/N = 20.57 and the experimental values are 1.68 and 22.2, respectively, which showed close agreement. In CPMTC assuming the grafting density for thiophene as 65% and 35% for carbazole, the calculated theoretical value is S/N = 4.59, but the experimental value was found to be S/N = 3.92. It is possible that more carbazole containing precursor polymers were incorporated in the film. However, XPS alone cannot reveal the extent of cross-linking in the system, and therefore detailed studies are underway to understand and possibly distinguish more complicated behavior in terms of their inter- vs intramolecular cross-linking.

AFM Analysis. Interesting features of these films also relate to the morphology of the electropolymerized films at different cycles. The cross-linked film average thickness was characterized using AFM profilometry measurements (see Supporting Information, Figure 2). The CPHC and CPMTC cross-linked polymer average film thicknesses after 15 CV cycles were found to be 110 and 95 nm, respectively. Figure 6a,b shows the CPHC, CPMTC, and CPHT cross-linked films after five CV cycles. The CPHC after five cycles showed a relatively rough morphology with rms roughness of 5.7 nm as compared to that of CPMTC, which showed more porous morphological features. Last, the CPHT cross-linked homopolymer shows (Figure 6c) a very rough and patchy film which was nonuniform macroscopically. These observations also correlated with the optical transparency of the CPHC and CPMTC films as compared to the opaque CPHT film. Since these measurements were taken on the initial stages of the film formation after five CV cycles, the observed morphologies can be related to the nucleation process as well as the effects of mass ion transport. The fact that the CPHC has a lower oxidation potential and linear CV deposition behavior suggests a rapid 3-D nucleation growth. For CPMTC

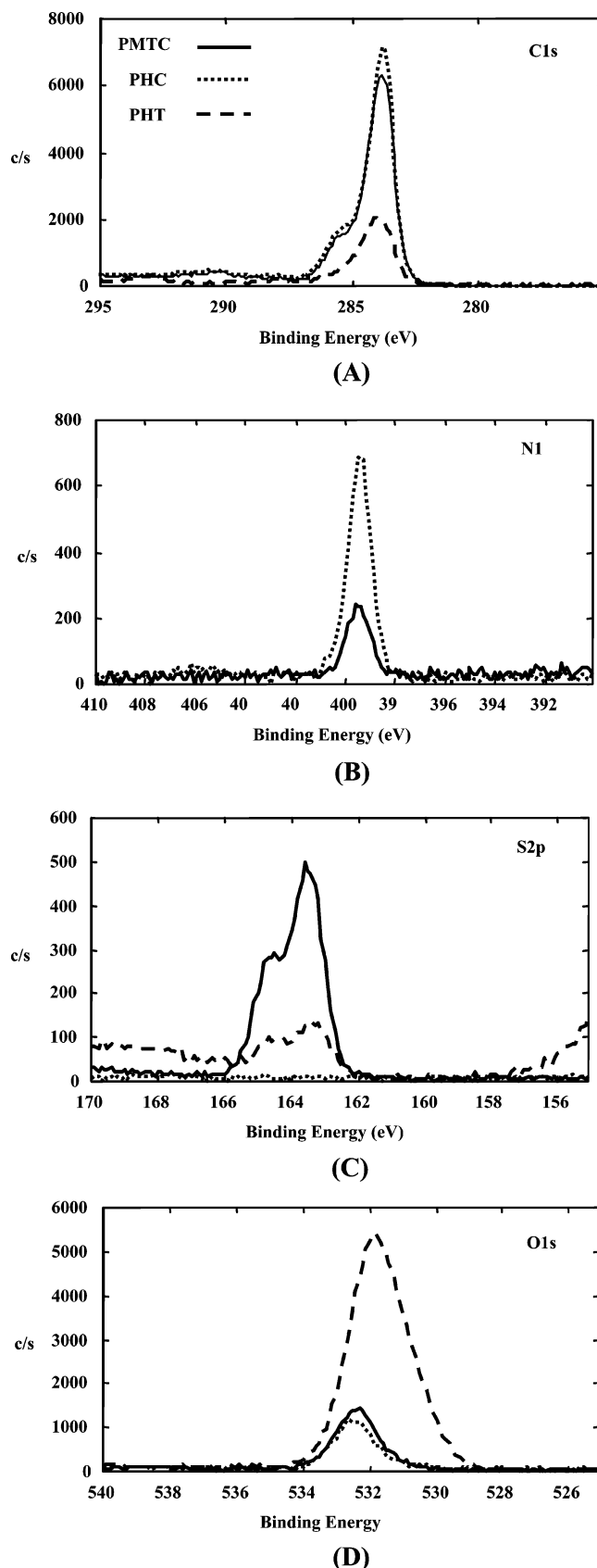


Figure 5. High-resolution XPS spectra of the cross-linked polymers: (A) C 1s, (B) N 1s, (C) S 2p, and (D) O 1s.

the porous structure is believed to be due to presence of more linear thiophene, facilitating better ion transport. In previous studies done on thiophene copolymers, similar trends in terms of morphologies were observed²⁷

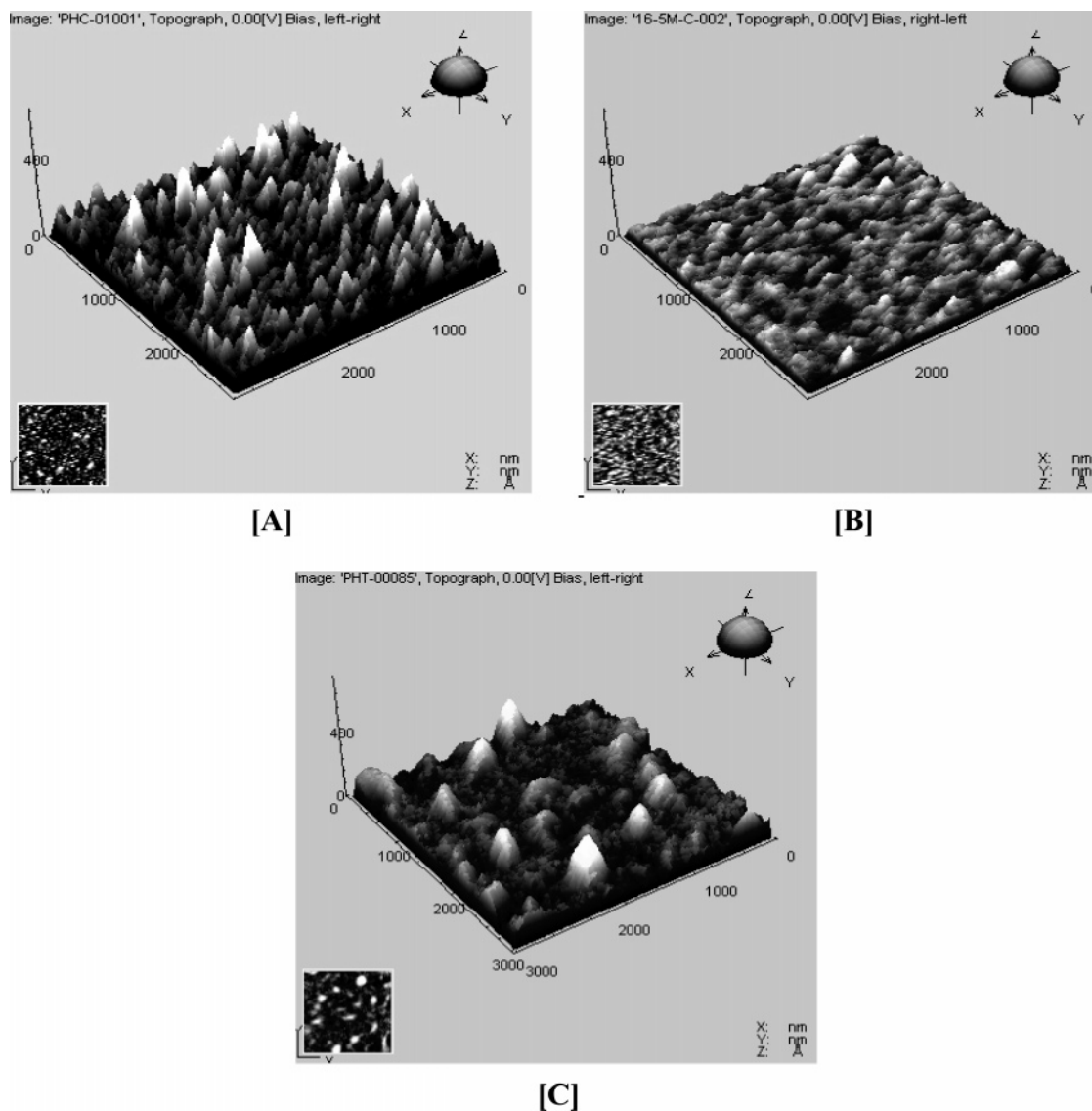


Figure 6. ($3 \times 3 \mu\text{m}^2$) 3D atomic force microscopy of the cross-linked precursor polymer after five CV cycles: [A] CPHC, [B] CPMTc, and [C] CPHT.

Table 1. High-Resolution XPS Spectra of the Cross-Linked Precursor Polymers

precursor polymers	C_{1s}^{25}		N_{1s}^{25}		S_{2p}^{26}	
	BE (eV)	AC	BE (eV)	AC	BE (eV)	AC
PHT	284.8 (C–C, C–H)	32.62			163.6 ($2p_{3/2}$) 164.8 ($2p_{1/2}$)	1.04
PHC	284.8 (C–C) 286.4 (C–N, C–O)	88.55	398.8 (N–C)	3.98		
PMTC	284.8 (C–C) 286.4 (C–N, C–O)	86.90	398.8 (N–C)	1.25	163.6 ($2p_{3/2}$) 164.8 ($2p_{1/2}$)	4.90

and were related to 3D disordered structures. Since the CPHT was hardly polymerized electrochemically, it was not surprising to see a patchy morphology resulting from incoherent deposition of the homopolymer. Last, correlation with the CV and electro-QCM studies and the XPS results confirms this copolymer behavior. The fact that the CPMTc was well-behaved in terms of linear film growth, uniform ion transport, and high incorporation of copolymer units results into films with high uniformity and optical transparency. Further studies will be made on these polymers as it relates to potentiostatic deposition methods. OLED applications studies toward ITO hole-transport layers are underway.^{6b}

Conclusion

In this investigation, two different pendent electroactive monomers (carbazole and thiophene) were grafted onto a polymer to form precursor copolymer with a binary composition. Homopolymers were also synthesized for comparative studies. The precursor polymers were electrochemically polymerized anodically by CV to study the cross-linking behavior and CPN film formation. The homoprecursor polymers showed good electropolymerizability for the carbazole but not for the thiophene. However, the copolymer showed very good electropolymerizability which showed incorporation of thiophene and carbazole units, and the films were

macroscopically transparent. Blends of the two homopolymers also showed electropolymerizability but formed opaque films and required higher potentials to deposit. The mechanism involved a “trigger” effect for the thiophenes based on the initial oxidation of the carbazole units in a radical cation to neutral monomer reaction pathway. Both copolymer and homopolymer electropolymerizations resulted in statistical intramolecular and intermolecular reaction between individual polymer chains, resulting in templating and cross-linking. This was verified by CV, spectroelectrochemistry, and XPS measurements. The morphology of the films correlated well with the deposition behavior.

Acknowledgment. The authors of this paper thank the partial funding from the Robert Welch Foundation (E-1551), NSF-DMR (99-8820110), NSF-DMR (0315565), and NSF-CTS (0330127). We also thank Dr. Paul A. W. van der Heide for XPS and Jason Locklin and Derek Patton for AFM profilometry and GPC measurements.

Supporting Information Available: EQCM studies, band gap/scan rate, and AFM profilometry measurements. This material is available free of charge via the Internet at <http://pubs.acs.org>.

References and Notes

- (1) (a) Bernier, P.; Lefrant, S.; Bidan, G., Eds.; *Advances in Synthetic Metals: Twenty Years of Progress in Science and Technology*; Elsevier: Lausanne, 1999. (b) Leclerc, M.; Faïd, K. *Adv. Mater.* **1997**, *9*, 1087–1094. (c) Leclerc, M. *J. Polym. Sci., Part A: Polym. Chem.* **2001**, *39*, 2867–2873. (d) Hupey, M. A.; Ober, C. K. *J. Vac. Sci. Technol.* **1998**, *16*, 3701–3704. (e) Li, Y.; Vamvounis, G.; Holderoft, S. *Macromolecules* **2002**, *35*, 6900–6906. (f) Fukukawa, K.; Shibasaki, Y.; Ueda, M. *Macromolecules* **2004**, *37*, 8256–8261. (g) Katz, H. E. *Chem. Mater.* **2004**, *16*, 4748–4756. (h) Veres, J.; Ogier, S.; Lloyd, G.; de Leeuw, D. *Chem. Mater.* **2004**, *16*, 4543–4555.
- (2) (a) Roncali, J. *Chem. Rev.* **1992**, *92*, 711–738. (b) Chan, H.; Ng, S. *Prog. Polym. Sci.* **1998**, *23*, 1167–1231. (c) Roncali, J. *Chem. Rev.* **1997**, *97*, 173–206. (d) Schopf, G.; Kossmehl, G. *Polythiophenes-Electrically Conducting Polymers*; Springer-Verlag: Berlin, 1997. (e) Kulkarni, A. P.; Tonzola, C. J.; Babel, A.; Jenekhe, S. A. *Chem. Mater.* **2004**, *16*, 4556–4573. (f) Thomas, C. A.; Zong, K.; Abboud, K. A.; Steel, P. J.; Reynolds, J. R. *J. Am. Chem. Soc.* **2004**, *126*, 16440–16450.
- (3) (a) McCullough, R. D.; Ewbank, P. C.; Loewe, R. S. *J. Am. Chem. Soc.* **1997**, *119*, 633–634. (b) Morin, J. F.; Leclerc, M. *Macromolecules* **2002**, *35*, 8413–8417. (c) Ballav, N.; Biswas, M. *Synth. Met.* **2003**, *132*, 213–218.
- (4) (a) Sotzing, G. A.; Reynolds, J. R.; Steel, P. J. *Chem. Mater.* **1996**, *8*, 882–889. (b) Geissler, U.; Hallensleben, M. L.; Rhode, N. *Synth. Met.* **1997**, *84*, 173–174. (c) Curtis, M. D.; McClain, M. D. *Chem. Mater.* **1996**, *8*, 936–944.
- (5) (a) Deng, S.; Advincula, R. *Chem. Mater.* **2002**, *14*, 4073–4080. (b) Taranekar, P.; Fan, X.; Advincula, R. *Langmuir* **2002**, *18*, 7943–7952. (c) Xia, C.; Fan, X.; Park, M.; Advincula, R. *Langmuir* **2001**, *17*, 7893–7898. (d) Inaoka, S.; Advincula, R. *Macromolecules* **2002**, *35*, 2426–2428. (e) Park, M.-K.; Xia, C.; Advincula, R. C.; Schutz, P.; Caruso, F. *Langmuir* **2001**, *17*, 7670–7674.
- (6) (a) Xia, C.; Advincula, R. C.; Baba, A.; Knoll, W. *Chem. Mater.* **2004**, *16*, 2852–2856. (b) Baba, A.; Onishi, K.; Knoll, W.; Advincula, R. C. *J. Phys. Chem. B* **2004**, *108*, 18949–18955. (c) Inaoka, S.; Roitman, D.; Advincula, R. In *Forefront of Lithographic Materials Research*; Ito, H., Khojasteh, M., Li, W., Eds.; Kluwer Academic Publishers: New York, 2001; pp 239–245.
- (7) Romero, D. B.; Schaer, M.; Zuppiroli, L.; Leclerc, M.; Adès, D.; Siove, A. *Synth. Met.* **1996**, *80*, 271–277.
- (8) (a) Faid, K.; Leclerc, M. *J. Am. Chem. Soc.* **1998**, *120*, 5274–5278. (b) Kumpumbu-Kalemba, L.; Leclerc, M. *Chem. Commun.* **2000**, *19*, 1847–1848. (c) Ho, H. A.; Boissinot, M.; Bergeron, M. G.; Corbeil, G.; Dore, K.; Boudreau, D.; Leclerc, M. *Angew. Chem., Int. Ed.* **2002**, *41*, 1548–1551. (d) McQuade, D. T.; Pullen, A. E.; Swager, T. M. *Chem. Rev.* **2000**, *100*, 2537–2574.
- (9) (a) Welzel, H.-P.; Kossmehl, G.; Boettcher, H.; Engelmann, G.; Hunnius, E.-D. *Macromolecules* **1997**, *30*, 7419–7426. (b) Svecjean, W. R.; Fréchet, M. J. *Polymer* **1990**, *31*, 165–174. (c) Sanda, F.; Kawaguchi, T.; Masuda, T.; Kobayashi, N. *Macromolecules* **2003**, *36*, 2224–2229. (d) Sanda, F.; Nakai, T.; Kobayashi, N.; Masuda, T. *Macromolecules* **2004**, *37*, 2703–2708.
- (10) (a) Sezer, E.; Ustamehmetoglu, B.; Saraç, A. S. *Synth. Met.* **1999**, *107*, 7–17. (b) Geiler, U.; HallenslebenLevent Toppare, M. L. *Synth. Met.* **1993**, *55*, 1483–1488.
- (11) (a) Ambrose, J. F.; Carpenter, L. L.; Nelson, R. F. *J. Electrochem. Soc. Electrochem. Sci. Technol.* **1975**, *122*, 7, 876–880. (b) Mengoli, G.; Musiani, M. M.; Schreck, B.; Zecchin, S. *J. Electroanal. Chem.* **1988**, *246*, 73–86.
- (12) Magnus, P.; Friend, R.; Greenham, N. *Adv. Mater.* **1998**, *10*, 769–774.
- (13) Colthup, N. B. *Introduction to Infrared & Raman Spectroscopy*, 2nd ed.; Academic Press: New York, 1975.
- (14) Sezer, E.; Hooren, V. M.; Sarac, S. A.; Hallensleben, L. M. *J. Polym. Sci., Part A: Polym. Chem.* **1999**, *37*, 379–381.
- (15) (a) Diaz, A. F.; Castillo, J.; Kanazawa, K. K.; Logan, J. A.; Salmon, M.; Fajardo, O. *J. Electroanal. Chem.* **1982**, *133*, 233–239. (b) Belletete, M.; Bedard, M.; Durocher, G. *Synth. Met.* **2004**, *146*, 99–108.
- (16) (a) Springer, J.; Sarac, S. A. *Surf. Coat. Technol.* **2002**, *160*, 227–238. (b) Sezer, E.; Sarac, S. A. *Int. J. Polym. Mater.* **2004**, *53*, 79–94.
- (17) Baba, A.; Knoll, W. *J. Phys. Chem. B* **2003**, *107*, 7733–7738.
- (18) Abe, Y.; Bernede, J.; Delvalle, A. M.; Tregouet, Y.; Diaz, R.; Lefrant, S. *Synth. Met.* **2002**, *126*, 1–6.
- (19) Hayashida, S.; Sukegawa Osamu, K. N. *Synth. Met.* **1990**, *35*, 253–261.
- (20) Kessel, R.; Schultz, W. *J. Surf. Interface Anal.* **1990**, *16*, 401–406.
- (21) Varghese, M. M.; Basu, T.; Malhotra, B. D. *Mater. Sci. Eng. C* **1995**, *3*, 215–218.
- (22) Zotti, G.; Schiavon, G.; Zecchin, S.; Morin, J. F.; Leclerc, M. *Macromolecules* **2002**, *35*, 2122–2128.
- (23) Baker, C.; Reynolds, J. R. *J. Electroanal. Chem.* **1987**, *251*, 307–322.
- (24) (a) Baba, A.; Tian, S.; Stefani, F.; Xia, C.; Wang, Z.; Advincula, R.; Johannsmann, D.; Knoll, W. *J. Electroanal. Chem.* **2004**, *562*, 95–103. (b) Baba, A.; Kaneko, F.; Advincula, R. C. *Colloids Surf. A* **2000**, *173*, 39–49.
- (25) Weng, L.-T.; Wong, P. C. L.; Ho, K.; Wang, S.; Zeng, Z.; Yang, S. *Anal. Chem.* **2000**, *72*, 4908–4913.
- (26) Soudan, P.; Lucas, P.; Breau, L.; Belanger, D. *Langmuir* **2000**, *16*, 4362–4366.
- (27) Kumru, E. M.; Springer, J.; Sarac, S. A.; Bismarck, A. *Synth. Met.* **2001**, *123*, 391–401.

MA050001H